



Evolution of beryllium microstructure under high-dose neutron irradiation

V.P. Chakin *, Z. Ye Ostrovsky

State Scientific Center of Russian Federation, Research Institute of Atomic Reactors 433510, Dimitrovgrad, Ulyanovsk region, Russia

Abstract

Beryllium is an advantageous material from the point of its usage in some components of perspective fusion reactors, such as reactor wall, divertor and blanket. The character of the microstructure change under neutron irradiation of beryllium is a determining factor in understanding of the processes resulting in the degradation of physical–mechanical properties of the material. The performed examinations of the TE-56 beryllium grade irradiated in the SM-reactor at 70–120 °C up to fluences of 2.5×10^{22} to 5.7×10^{22} cm⁻² ($E > 0.1$ MeV) and TE-400 beryllium grade irradiated in the BOR-60 reactor at 400 °C up to a fluence of 1.6×10^{23} cm⁻² ($E > 0.1$ MeV) demonstrated that low-temperature irradiation resulted in the generation of dislocation loops and high-temperature irradiation resulted in the generation of plane hexahedral voids in a basal plane. The effect of short-term high-temperature annealing on the microstructure after low-temperature irradiation is studied also. One hour anneal at 300–1200 °C gives rise to loops and results in their evolution in dislocation network as well as generation and growing of the gas bubbles.

© 2002 Published by Elsevier Science B.V.

1. Introduction

Beryllium exhibits the unique physical–mechanical and neutron-physical properties and therefore it is supposed to be used as material of some components of perspective fusion reactors. Specifically, it is supposed to be used as material facing plasma in the ITER first wall structure and the divertor. Moreover, it is supposed to be used as neutron-multiplying material in the DEMO reactor blanket [1]. Neutron irradiation results in the degradation of beryllium properties. The neutron dose increase causes its embrittlement, swelling and loss of heat conductivity, etc. [2–4]. Considerable changes in microstructure provide the basis for deterioration of beryllium properties, which occurred in material bombardment with high-energy neutrons. Particularly, neutron irradiation of beryllium leads to elastic and inelastic interaction of neutrons with the matrix atoms. Gas

atoms (helium, tritium) are generated in large quantities as a result of threshold neutron-beryllium reactions along with disturbance of beryllium atoms from equilibrium to form radiation-induced defects such as dislocation loops [5]. Mainly, these microstructure effects characterize the change in macroproperties of irradiated beryllium.

The present paper presents the results of beryllium microstructure examinations using metallography and transmission electron microscopy (TEM) techniques. The beryllium was irradiated up to high neutron doses in the SM and BOR-60 reactors.

2. Materials and examination technique

The disk specimens to be 3 mm in diameter and 0.3–0.4 mm in thickness intended for TEM examinations were made from beryllium product fragments after their operation in the SSC RF RIAR reactors using the electrical erosion technique. The beryllium products were operated and irradiated in contact with the primary water coolant of the SM reactor or in helium medium of commercial grade in the BOR-60 reactor. Table 1

* Corresponding author. Tel.: +7-84235 32021; fax: +7-84235 35648.

E-mail address: bond@niiar.ru (V.P. Chakin).

Table 1
Irradiation parameters of examined beryllium specimens

Reactor	Beryllium product	Location of the cutout fragment	Irradiation parameters			
			Medium	Temperature (°C)	Fluence (cm ⁻²) ($E > 0.1$ MeV)	Helium content (at. ppm)
SM	Neutron trap insert	Middle plane of the core	Water	70–120	5.7×10^{22} , 2.5×10^{22}	11 500, 5050
BOR-60	Neutron source	Middle plane of the core	Helium	400	16	9800

Table 2
Some characteristics of the examined beryllium grades

Grade	Fabrication method	Maximal grain size (μm)	Basic component content (%mass)		
			Be	O	BeO
TE-56	Hot extrusion	56	98.6	0.98	1.48
TE-400	Hot extrusion	400	~97.8	~1.5	~2.2

presents the irradiation parameters for the examined specimens. Irradiation temperature and neutron fluences

were calculated. Further, some of the specimens were subject to vacuum annealing for 1 h at 300–1200 °C.

Table 2 includes some characteristics of the examined TE-56 grade (material of SM neutron trap insert) and TE-400 grade (BOR-60 neutron source material).

Metallographic examinations of specially etched specimens were performed using the optical microscope MIM-15. The specimens were prepared in an electrolyte containing methyl alcohol and acetic acid with the use of double jet installation for electron microscopy examinations. The JEM-2000FXII electron microscope was

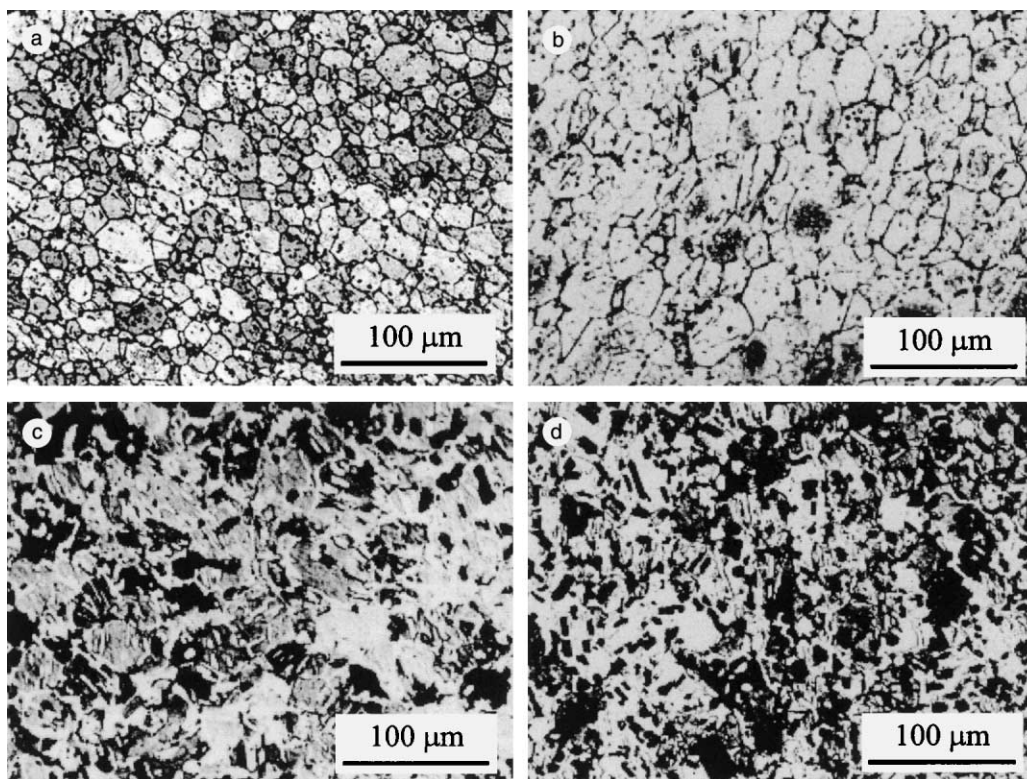


Fig. 1. Metallographic examinations of the TE-56 beryllium grade irradiated in the SM reactor up to 5.7×10^{22} cm⁻² ($E > 0.1$ MeV) at 70–120 °C: (a) after irradiation; (b) irradiation + annealing at 600 °C, 1 h; (c) irradiation + annealing at 800 °C, 1 h; (d) irradiation + annealing at 1000 °C, 1 h.

used for the specimen examination. The accelerating voltage was 120 kV.

3. Experimental data

3.1. High-temperature annealing effects on microstructure evolution of beryllium irradiated at 70–120 °C

Fig. 1 demonstrates the results of metallographic examinations on irradiated beryllium. The state after irradiation (Fig. 1(a)) when the grains of the base metal and second phase inclusions are present does not differ from the initial one in the range of 100 μm . The contrast of separate grains begins to change with increase in annealing temperature up to 600 °C (Fig. 1(b)) that involves the redistribution of helium atoms within the grain boundaries. Further increase in annealing temperature up to 800 °C (Fig. 1(c)) leads to typical structure forming where the prolate gas bubbles are present in great amount. The size and quantity of gas bubbles increase considerably after annealing at 1000 °C.

The dislocation structure of these particular specimens is shown in Fig. 2. The specimen state after irradiation (Fig. 2(a)) is characterized by the presence of

dislocation loops, the average size is 20 nm and bulk density is $3.1 \times 10^{15} \text{ cm}^{-3}$. The precise examinations associated with the fixed change in specimen location relative to the electron beam demonstrate that the loops are of interstitial type. The character of the loop distribution throughout the structure is extremely non-uniform. Particularly, there are regions that are free from loops. At an annealing temperature of 300 °C (Fig. 2(b)) the dislocation loops take the prolate ellipsoid shape, their size increases considerably (approximately up to 80–100 nm) and the bulk density decreases significantly. At least two planes of location are seen one of which is the basal plane. The increase in annealing temperature up to 500 °C (Fig. 2(c)) causes further growing of loops, which evolve gradually into the dislocation network.

No helium was found during the examinations of irradiated specimens even after the subsequent anneals at temperatures of 300 and 400 °C in spite of its considerable amount in the material (see Table 1). This depends on the fact that helium atoms are present as subatomic complexes, which are indistinguishable when the TEM technique is used. First smallest gas bubbles defined with the electron microscope appear when the annealing temperature is 500 °C (Fig. 3(a)). They are sized to be 1–4 nm. The bulk density is $3.5 \times 10^{17} \text{ cm}^{-3}$.

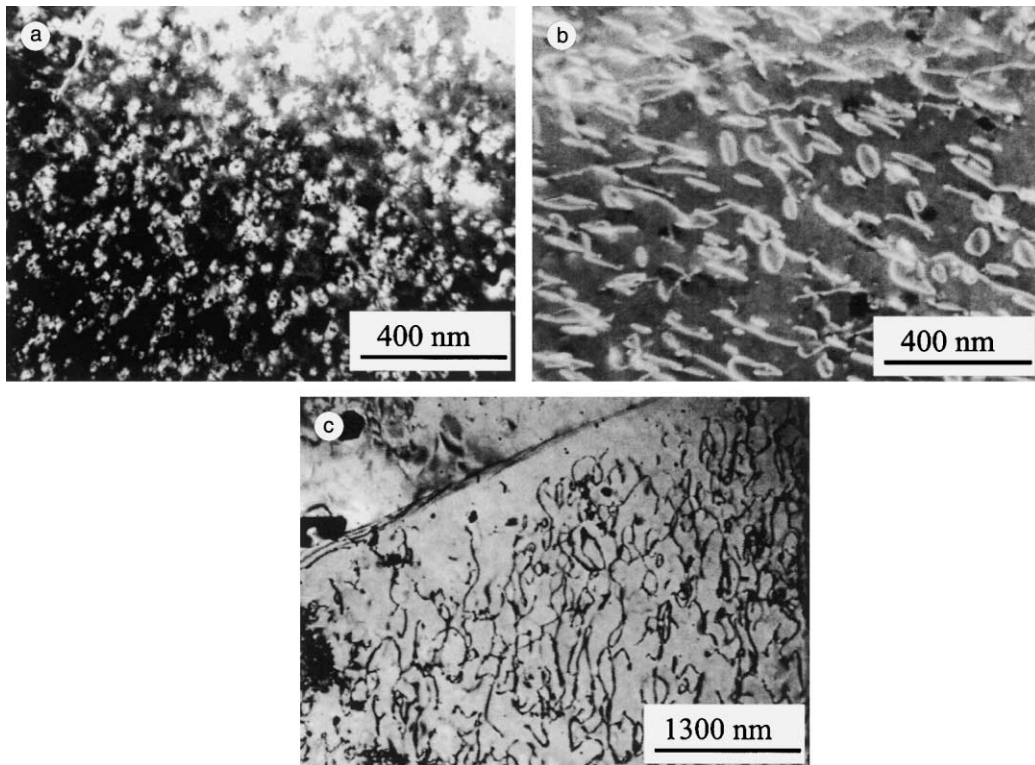


Fig. 2. Dislocation structure of the TE-56 beryllium grade irradiated in the SM reactor up to $2.5 \times 10^{22} \text{ cm}^{-2}$ ($E > 0.1 \text{ MeV}$) at 70–120 °C: (a) after irradiation; (b) irradiation + annealing at 300 °C, 1 h; (c) irradiation + annealing at 500 °C, 1 h.

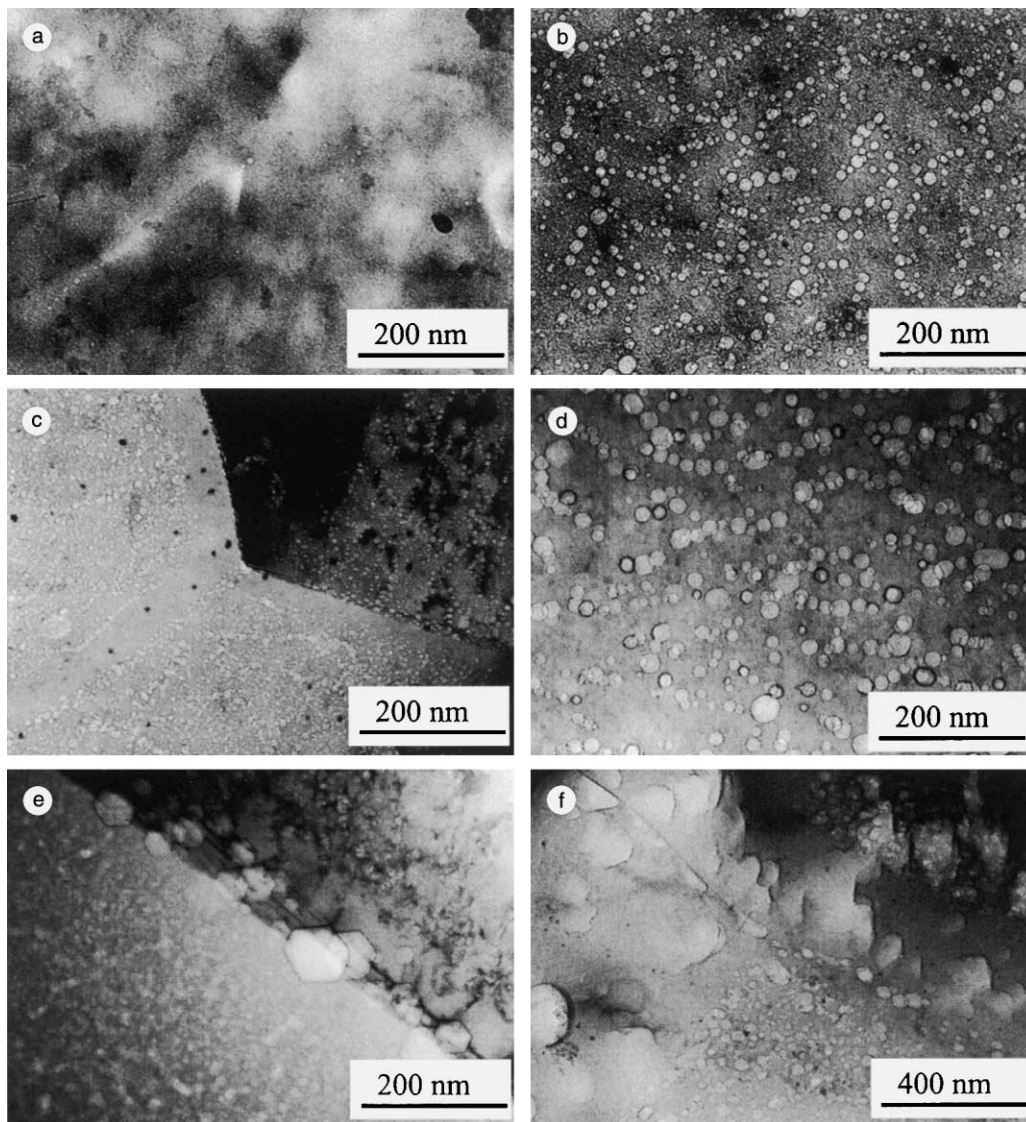


Fig. 3. Evolution of gas bubbles in the TE-56 beryllium grade irradiated in the SM reactor up to $2.5 \times 10^{22} \text{ cm}^{-2}$ ($E > 0.1 \text{ MeV}$) at 70–120 °C after high-temperature annealing: (a) 500 °C, 1 h; (b) 700 °C, 1 h; (c) 1000 °C, 1 h; (d) 1200 °C, 1 h.

The distribution of gas bubbles over the structure is uniform. Usually they form chains along the dislocation generations such as low angle boundaries and separate dislocations. The average size of bubbles grows up to 12 nm and the bulk density goes down to $2.2 \times 10^{16} \text{ cm}^{-3}$ with an increase in annealing temperature up to 700 °C (Fig. 3(b)). In most cases the gas bubbles form the extended chains. The broad depletion regions (Fig. 3(b)) are seen along grain boundaries. The boundaries themselves are filled with gas bubbles of nearly the same size as those in the matrix, but the separate grain-boundary bubbles to be 20 nm in size occur. The grain size grows up further up to 20 nm and the density goes down to

$7.3 \times 10^{15} \text{ cm}^{-3}$ at an annealing temperature of 1000 °C (Fig. 3(c)). Gas bubbles at the boundaries are often of larger size than those in the matrix. Sometimes their mean diameter is 50 nm (Fig. 3(d)). The hexahedral shape is defined when the bubbles are considerable in size. But it is clear that this is a volumetric formation rather than a plane formation. There are bubbles of the size of 25 nm at annealing temperature of 1200 °C (Fig. 3(d)). The other places are occupied with craters of microbubbles. Comparison between the metallographic and TEM data reveals that the generation of very big gas bubbles takes place at an annealing temperature of 800 °C according to the data obtained with the use of the

metallographic technique but the bubbles are absent at all at the same temperature according to the TEM data. Probably, such difference can be explained by different neutron doses, which have been accumulated on these particular specimens (see Table 1).

3.2. Microstructure of beryllium irradiated at 400 °C

As the TE-400 beryllium grade was used in the nuclear reactor industry in the 1960s its quality does not meet the modern requirements. Fig. 4 shows the metallographic microstructure. It is obvious that the grains are extremely non-uniform in size. Moreover, the material contains impurities in high amount (see Table 2). Fig. 5(a) can be used as visual proof. It demonstrates the general view of the specimen area subjected to the examination with the use of electron microscopy. Fig. 5(b) demonstrates the boundary, which is filled with gas bubbles to be up to 400 nm in size. There are depletion regions along the boundaries and as for the grain body, the radiation-induced defects are found here, which in turn can be characterized as plain voids. Voids lie down in the basal planes, therefore their shape at the picture section depends on the grain orientation relative to this particular cross-section. Fig. 5(c) shows voids at the cross-section, which is perpendicular to the basal plane and Fig. 5(d) shows the voids at the cross-section, which is parallel with it. The voids take a rather regular hexahedral shape therefore they can be named as short hexagonal prisms. The mean distance between the opposite sides is 50 nm, voids are 5–10 nm in thickness and the bulk density is $8.5 \times 10^{15} \text{ cm}^{-3}$. The chains of gas bubbles to be up to 60 nm in size (Fig. 5(e)) are noticed along the structure defects such as dislocations and low angle sub-boundaries.

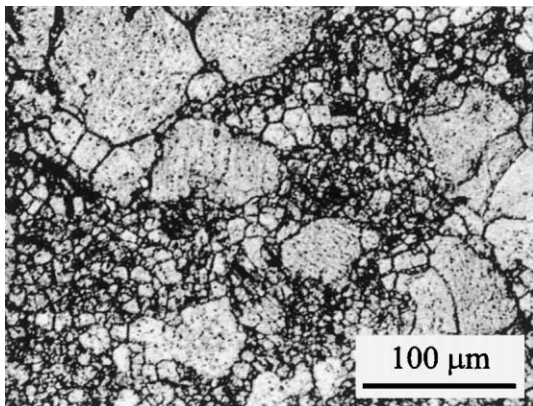


Fig. 4. Metallography of the TE-400 beryllium grade irradiated in the BOR-60 reactor up to $1.6 \times 10^{23} \text{ cm}^{-2}$ ($E > 0.1 \text{ MeV}$) at 400 °C.

4. Discussion

The irradiated beryllium microstructure was examined using transmission electron microscopy at the beginning of 1960s. But right now the character of defect formation according to the processing characteristics of the material used and irradiation conditions has not been studied properly. Some experimental data are rather contradictive but there are also some alternative versions of data interpretation. Ref. [6] gives an overview of the status of work under this problem. Particularly, it is mentioned that gas bubbles are absent at all in irradiated beryllium at irradiation temperatures below 200 °C because the diffusive mobility of separate helium atoms or helium-based complexes is insufficient for displacement at distances sufficient for generation of rather big gas atom clusters at this particular temperature. The post-irradiation high-temperature annealing helps to reveal helium absence in the material, which redistributes over the structure during annealing and causes the generation of gas bubbles along the boundaries and in the grain body. Sometimes the radiation-induced defects [7] are absent at all in the beryllium structure after low-temperature annealing. Sometimes there is information relating to the dislocation loops or clusters [8]. We believe that the dislocation loops should be always present in beryllium at low irradiation temperatures although they can be distributed throughout the structure non-uniformly. The preparation of irradiated specimens for examination is complicated because of its high degree of brittleness and a limited number of places transparent for electron beam. More than that it is true for majority of performed examinations that the low neutron dose can be insufficient for the generation of displaced matrix atoms in considerable amount.

The present work defines the presence of interstitial dislocation loops in irradiated beryllium for sure because the examined specimens have been irradiated up to high neutron fluences at temperatures of 70–120 °C. It was proved that the first gas bubbles distinguishable by the electron microscopy appear only after annealing at 500 °C for 1 h and when the neutron fluence is $2.5 \times 10^{22} \text{ cm}^{-2}$ ($E > 0.1 \text{ MeV}$). A further increase in annealing temperature leads to bubble growth and bulk density reduction correspondingly. Moreover, the bubbles manage to preserve the bulk shape that points to the equality of all crystallographic directions and planes in the diffusion displacement of helium atoms towards the growing gas bubble.

According to the published data the neutron irradiation of beryllium over the temperature range 350–480 °C leads to the formation of radiation-induced plane defects, which find their places in the grain body as well as it leads to the generation of grain-boundary gas bubbles. This formation in the grain body is identified as plane clusters of defects taking the form of c-type loops,

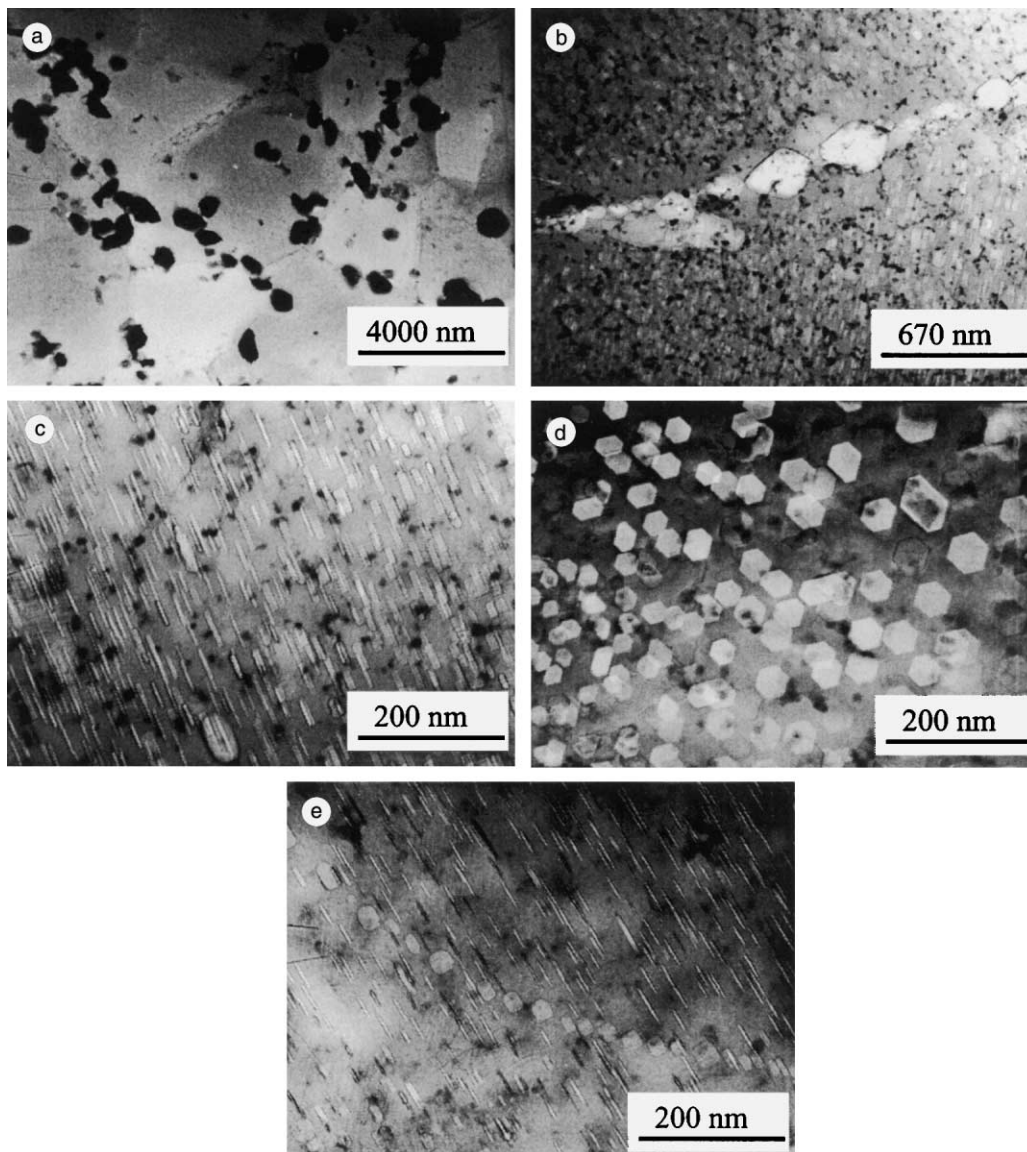


Fig. 5. Microstructure of the grade TE-400 beryllium irradiated in the BOR-60 reactor up to $1.6 \times 10^{23} \text{ cm}^{-2}$ ($E > 0.1 \text{ MeV}$) at $400 \text{ }^\circ\text{C}$: (a) general view of inclusion particles in the second phases; (b) gas bubbles along the grain boundaries; (c) and (d) different projections of plane gas voids; (e) chain of gas bubbles.

which are found in the basal plane [9,10]. According to the assumption made in [11] the helium segregation into the c-type loops results in the formation of plane gas bubbles.

This plane formation is identified as stacking fault dislocations [6]. The present work reveals that the flat formation takes the shape of short hexahedral prisms which can be characterized as flat hexahedral voids pain down in the basal plane due to the fact that beryllium has been irradiated by neutrons up to significantly higher doses rather than it has been done in the above-

mentioned work. We believe that the mechanism of their formation is associated not only with diffusion but with the radiation-induced segregation of helium in sinks, which are the dislocation loops preserving the thermal stability. The presence of displaced matrix atoms in large quantity leads to a vacancy oversaturation of the material, therefore free vacancies take part in the plane void formation. As a result there is a gradual evolution of dislocation loops into voids having the considerable gas filling. This particular mechanism differs from the mechanism of gas bubble generation in the course of

short-term annealing of beryllium (irradiated at low temperature) at 400–600 °C by the presence of radiation-induced defects such as helium segregation in loops, vacancy oversaturation of matrix and probably some other as well. Taken together these factors complicate the thermal diffusion, which proceeds in the irradiated specimen in annealing and causes the preference of gas atom fluxes in some crystallographic directions and their preferential deposition in the basal plane in the form of dislocation loops, correspondingly.

5. Conclusion

The microstructure of the TE-56 beryllium grade irradiated in the SM reactor up to fluences of 2.5×10^{22} to $5.7 \times 10^{22} \text{ cm}^{-2}$ ($E > 0.1 \text{ MeV}$) at 70–120 °C and TE-400 beryllium grade irradiated in the BOR-60 reactor up to fluence of $1.6 \times 10^{23} \text{ cm}^{-2}$ ($E > 0.1 \text{ MeV}$) at 400 °C was subject of examination. Neutron irradiation leads to dislocation loop formation at 70–120 °C. The growth of loops and their evolution in the dislocation network as well as generation and growing of gas bubbles take place in the course of post-irradiation annealing at 300–1200 °C for 1 h. The first gas bubbles have been noticed at an annealing temperature of 500 °C. Irradiation at 400 °C results in the formation of plane hexahedral voids, which lie down in the basal plane. The formation mechanism consists in the combination of processes such as radiation-induced helium segregation and helium diffusion as well as vacancy sinking in loops as the defect sinks.

References

- [1] F. Scaffidi-Argentina, G.R. Longhurst, V. Shestakov, H. Kawamura, *J. Nucl. Mater.* 283–287 (2000) 43.
- [2] V. Barabash, G. Federici, M. Rödiger, L.L. Snead, C.H. Wu, *J. Nucl. Mater.* 283–287 (2000) 138.
- [3] V.P. Chakin, I.B. Kupriyanov, V.A. Tsykanov, V.A. Kazakov, R.R. Melder, Swelling and mechanical properties of beryllium irradiated in the SM reactor at low temperature, in: *Proceedings of the 4th IEA International Workshop on Beryllium Technology for Fusion*, 15–17 September 1999, Karlsruhe, Germany, April 2000, p. 257.
- [4] V.P. Chakin et al., High dose neutron irradiation damage in beryllium as blanket material, *Fus. Eng. Des.* 58&59 (2001) 535.
- [5] V.P. Goltsev, G.A. Sernyaev, Z.I. Chechetkina, *Radiation Material Science of Beryllium*, Science and Engineering, Minsk, 1977.
- [6] L. Coheur, J.-M. Cayphas, P. Delavignette, M. Hou, Microstructural effects of neutron irradiation in beryllium, in: *Proceedings of the 4th IEA International Workshop on Beryllium Technology for Fusion*, 15–17 September 1999, Karlsruhe, Germany, April 2000, p. 247.
- [7] R.G. Fleck, *ASTM-STP 782* (1982) 735.
- [8] J.-M. Beeston, M.R. Martin, C.R. Brinkman, *CONF-730801* (1973) 59.
- [9] D.S. Gelles, H.L. Heinisch, *J. Nucl. Mater.* 191–194 (1992) 194.
- [10] M. Dalle Donne et al., *JAERI-CONF-98-001* (1998) 296.
- [11] D.S. Gelles, M. Dalle Donne, H. Kawamura, F. Scaffidi-Argentina, Microstructural examination of irradiated beryllium pebbles, in: *Proceedings of the 19th ASTM International Symposium on Effects of Radiation of Materials*, Seattle, USA, 16–18 June 1998.